Measurement of cosmic-ray antiproton spectrum at solar minimum with a long-duration balloon flight in Antarctica

K. Abe,[1,*] H. Fuke,[2] S. Haino,[3,†] T. Hams,[4] M. Hasegawa,[3] A. Horikoshi,[3] K. C. Kim,[5] A. Kusumoto,[1] M. H. Lee,[5] Y. Makida,[3] S. Matsuda,[3] Y. Matsukawa,[1] J. W. Mitchell,[4] J. Nishimura,[6] M. Nozaki,[3] R. Orito,[1,‡] J. F. Ormes,[7] K. Sakai,[6,§] M. Sasaki,[4] E. S. Seo,[5] R. Shinoda,[6] R. E. Streitmatter,[4] J. Suzuki,[3] K. Tanaka,[3] N. Thakur,[7] T. Yamagami,[2] A. Yamamoto,[3,6] T. Yoshida,[2] and K. Yoshimura[3]

[1]*Kobe University, Kobe, Hyogo 657-8501, Japan*
[2]*Institute of Space and Astronautical Science, Japan Aerospace Exploration Agency (ISAS/JAXA), Sagamihara, Kanagawa 229-8510, Japan*
[3]*High Energy Accelerator Research Organization (KEK), Tsukuba, Ibaraki 305-0801, Japan*
[4]*NASA-Goddard Space Flight Center (NASA-GSFC), Greenbelt,MD 20771, USA*
[5]*IPST, University of Maryland, College Park, MD 20742, USA*
[6]*The University of Tokyo, Bunkyo, Tokyo 113-0033, Japan*
[7]*University of Denver, Denver, CO 80208, USA*

(Dated: July 27, 2011)

The energy spectrum of cosmic-ray antiprotons ($\bar{p}$'s) has been measured in the range 0.17 to 3.5 GeV, based on 7886 $\bar{p}$'s collected by the BESS-Polar II instrument during a long-duration flight over Antarctica in the solar minimum period of December 2007 through January 2008. The $\bar{p}$ spectrum measured by BESS-Polar II shows good consistency with secondary $\bar{p}$ calculations. Cosmologically primary $\bar{p}$'s have been searched for by comparing the observed and calculated $\bar{p}$ spectra. The BESS-Polar II result shows no evidence of primary $\bar{p}$'s originating from the evaporation of PBH.

The precise measurement of the spectrum of cosmic-ray antiprotons ($\bar{p}$'s) is crucially important to investigations of conditions in the early universe and of cosmic-ray propagation. Most cosmic-ray $\bar{p}$'s are produced by energetic nuclear cosmic rays interacting with the interstellar gas. The energy spectrum of such "secondary" $\bar{p}$'s is expected to show a characteristic peak around 2 GeV, with sharp decreases of the flux below and above the peak due to the kinematics of $\bar{p}$ production and the interstellar proton spectrum. The secondary $\bar{p}$'s offer a unique probe [1–3] of cosmic-ray propagation and of solar modulation. Other possible sources of cosmic-ray $\bar{p}$'s have been sought, such as primordial black holes (PBH) evaporating by Hawking radiation [4]. The "primary" spectral contributions of PBH sources, if they exist, are expected to be observable at low energies [5] and to exhibit large solar modulation effects [6] due to the shape of the predicted spectrum.

In the previous solar minimum period, the BESS experiment (BESS95+97) showed that the $\bar{p}$ spectrum has a distinct peak around 2 GeV, as expected, and it has become evident that $\bar{p}$'s are predominantly of secondary origin [7]. However, the low-energy component of the $\bar{p}$ spectrum measured by BESS95+97 was slightly flatter than predicted by calculations with secondary $\bar{p}$ models. Though this result might suggest the existence of novel processes for production of cosmic-ray $\bar{p}$'s, the large statistical error of the BESS95+97 data did not allow a firm conclusion. The BESS-Polar project [8–10] was proposed to evaluate the possibility of excess low-energy $\bar{p}$ flux suggested in the BESS95+97 observation by measuring $\bar{p}$'s with unprecedented precision using long-duration flights over Antarctica at solar minimum. The flight of BESS-Polar I was performed in December 2004 [11–14] and the flight of BESS-Polar II [12] was carried out near solar minimum during December 2007 and January 2008. In this Letter, we report a new measurement of cosmic-ray $\bar{p}$'s in the energy range 0.17 GeV to 3.5 GeV by BESS-Polar II. Based on the measured spectrum, the subjects of secondary $\bar{p}$'s and possible primary $\bar{p}$'s are discussed.

The BESS-Polar instrument [15–17] was designed and developed as a high-resolution magnetic-rigidity spectrometer. A uniform field of 0.8 T is produced by a thin superconducting solenoid, and the field region is filled with drift-chamber tracking detectors. Tracking is performed by fitting up to 52 hit points with a characteristic resolution of $\sim 140\mu$m in the bending plane, resulting in a magnetic-rigidity ($\equiv Pc/Ze$) resolution of 0.4% at 1 GV and a maximum detectable rigidity (MDR) of 270 GV. Upper and lower scintillator hodoscopes provide time-of-flight (TOF) and dE/dx measurements and the event trigger. For antiproton measurements, the acceptance of BESS-Polar is 0.23 m^{2}sr. The timing resolution of the TOF system is 120 ps, giving a β^{-1} resolution of 2.5%. The instrument also incorporates a threshold-type Cherenkov counter using a silica aerogel radiator with index $n = 1.03$ (ACC) that can reject e^- and μ^- backgrounds by a factor of 6100 and distinguish $\bar{p}$'s from such backgrounds up to 3.5 GeV. In addition, a thin scintillator middle-TOF (MTOF) is installed on the lower surface of the solenoid bore to detect low-energy particles which cannot penetrate the magnet wall. The timing resolution using the MTOF is 320 ps. In the present analysis, the MTOF was employed to verify the procedure used to eliminate contamination from events in which interacting protons mimic low-energy $\bar{p}$'s.

TABLE I. $\bar{p}$ flux at the top of atmosphere with statistical (first) and systematic (second) errors. $N_{\bar{p}}$ and N_{BG} are the number of observed antiprotons and estimated background events.

Kinetic energy (GeV) range	Kinetic energy (GeV) mean	$N_{\bar{p}}$	N_{BG}	$\bar{p}$ flux ($m^{-2}sr^{-1}s^{-1}GeV^{-1}$)	Kinetic energy (GeV) range	Kinetic energy (GeV) mean	$N_{\bar{p}}$	N_{BG}	$\bar{p}$ flux ($m^{-2}sr^{-1}s^{-1}GeV^{-1}$)
0.17–0.23	0.20	29	0.0	$3.56^{+0.88+0.41}_{-0.78-0.41} \times 10^{-3}$	0.98–1.07	1.03	238	0.1	$1.75^{+0.15+0.13}_{-0.15-0.13} \times 10^{-2}$
0.23–0.27	0.25	26	0.0	$4.53^{+1.23+0.53}_{-1.10-0.53} \times 10^{-3}$	1.07–1.17	1.12	283	0.2	$1.91^{+0.15+0.14}_{-0.15-0.14} \times 10^{-2}$
0.27–0.32	0.30	38	0.0	$5.09^{+1.13+0.53}_{-1.03-0.53} \times 10^{-3}$	1.17–1.28	1.23	304	0.6	$1.82^{+0.14+0.13}_{-0.14-0.13} \times 10^{-2}$
0.32–0.37	0.35	69	0.0	$7.55^{+1.16+0.52}_{-1.07-0.52} \times 10^{-3}$	1.28–1.40	1.34	399	1.7	$2.28^{+0.15+0.16}_{-0.15-0.16} \times 10^{-2}$
0.37–0.41	0.39	44	0.0	$8.05^{+1.63+0.53}_{-1.49-0.53} \times 10^{-3}$	1.40–1.53	1.47	412	3.5	$2.07^{+0.14+0.14}_{-0.14-0.14} \times 10^{-2}$
0.41–0.44	0.42	56	0.0	$9.19^{+1.65+0.62}_{-1.42-0.62} \times 10^{-3}$	1.53–1.68	1.60	466	6.2	$2.10^{+0.14+0.14}_{-0.14-0.14} \times 10^{-2}$
0.44–0.48	0.46	68	0.0	$9.95^{+1.58+0.72}_{-1.46-0.72} \times 10^{-3}$	1.68–1.84	1.75	485	9.0	$1.91^{+0.13+0.13}_{-0.13-0.13} \times 10^{-2}$
0.48–0.53	0.50	87	0.0	$1.14^{+0.16+0.08}_{-0.15-0.08} \times 10^{-2}$	1.84–2.01	1.92	555	11.5	$2.05^{+0.13+0.13}_{-0.12-0.13} \times 10^{-2}$
0.53–0.57	0.55	84	0.0	$9.30^{+1.41+0.74}_{-1.32-0.74} \times 10^{-3}$	2.01–2.20	2.11	632	12.9	$2.18^{+0.12+0.14}_{-0.12-0.14} \times 10^{-2}$
0.57–0.63	0.60	122	0.0	$1.26^{+0.15+0.09}_{-0.14-0.09} \times 10^{-2}$	2.20–2.41	2.31	622	13.7	$1.88^{+0.11+0.12}_{-0.11-0.12} \times 10^{-2}$
0.63–0.68	0.65	131	0.0	$1.20^{+0.14+0.09}_{-0.13-0.09} \times 10^{-2}$	2.41–2.64	2.53	678	13.8	$1.95^{+0.11+0.12}_{-0.11-0.12} \times 10^{-2}$
0.68–0.75	0.71	154	0.0	$1.32^{+0.14+0.10}_{-0.14-0.10} \times 10^{-2}$	2.64–2.89	2.76	637	13.3	$1.77^{+0.10+0.11}_{-0.10-0.11} \times 10^{-2}$
0.75–0.82	0.78	157	0.0	$1.30^{+0.15+0.10}_{-0.14-0.10} \times 10^{-2}$	2.89–3.16	3.00	494	12.5	$1.90^{+0.12+0.20}_{-0.12-0.21} \times 10^{-2}$
0.82–0.89	0.86	209	0.0	$1.84^{+0.17+0.12}_{-0.16-0.12} \times 10^{-2}$	3.16–3.46	3.28	213	11.5	$1.64^{+0.18+0.20}_{-0.17-0.21} \times 10^{-2}$
0.89–0.98	0.94	194	0.0	$1.51^{+0.15+0.10}_{-0.14-0.10} \times 10^{-2}$					

The BESS-Polar II payload was launched on December 23, 2007, from Williams Field near the US McMurdo Station in Antarctica and circulated around the South Pole for 24.5 days of observation with the magnet energized. The float altitude was 34 km to 38 km (residual air of 5.8 g/cm^2 on average), and the cutoff rigidity was below 0.5 GV. BESS-Polar II accumulated 4.7×10^9 events with no inflight event selection as 13.6 terabytes of data.

During the flight, most detectors and instrument systems operated well and provided their expected performance. The central tracker exhibited high-voltage fluctuations. However, normal tracking resolution was obtained for more than 90% of the science observation time by development of algorithms that calibrate the tracker over short time intervals and depend on its high-voltage state. One upper TOF PMT and one lower TOF PMT had high-voltage control problems and were turned off. A conservative requirement of two good PMTs on each TOF scintillator resulted in a $\sim 20\%$ reduction in acceptance.

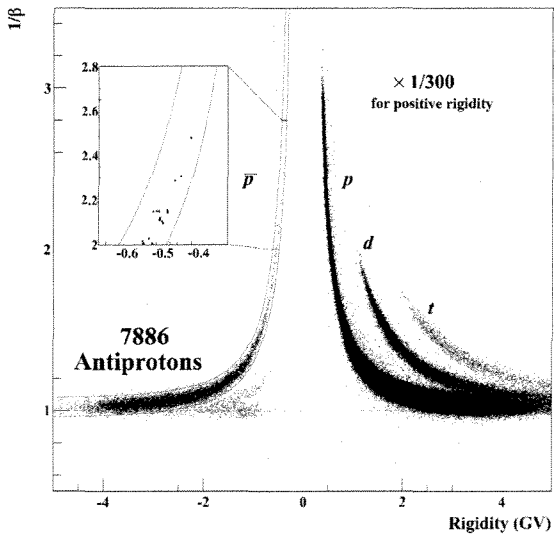

FIG. 1. The β^{-1} versus rigidity plot and $\bar{p}$'s selection band. The solid curves define the $\bar{p}$ mass bands. The lowest energy $\bar{p}$'s are shown in the closeup figure.

Analysis was performed in the same way as described in Ref. [7]. The same selection criteria for $\bar{p}$'s and protons were applied because noninteracting $\bar{p}$'s behave similarly to protons in the symmetrical configuration of BESS-Polar, except for deflection direction.

Figure 1 shows β^{-1} versus rigidity plots for surviving events. We see a clean narrow band of 7886 $\bar{p}$'s at the exact mirror position of the protons. The ACC veto helped identify $\bar{p}$ events at higher energies by removing the background of e^- and μ^-. The fractions of contamination were 0.0%, 1.0%, and 2.3% in the 0.2–1.0 GeV, 1.0–2.0 GeV, and 2.0–3.5 GeV energy bands. Other backgrounds such as albedo, mismeasured positive-rigidity particles, and re-entrant albedo were found to be negligible.

After $\bar{p}$ candidates are identified, the differential flux of $\bar{p}$'s at the top of atmosphere ($\Phi_{\rm TOA}$) integrated in an energy width of dE can be expressed as follows:

$$\Phi_{\rm TOA} {\rm d}E = (N_{\rm TOI} - N_{\rm atmos})/\varepsilon_{\rm air}/(S\Omega \cdot T_{\rm live}) \quad (1)$$

$$N_{\rm TOI} = (N_{\bar{\rm p}} - N_{\rm BG})/(\varepsilon_{\rm det} \cdot \varepsilon_{\rm non-int}) \quad (2)$$

where $T_{\rm live}$ is the live time, $N_{\bar{\rm p}}$ and $N_{\rm BG}$ are the numbers of observed $\bar{p}$ candidates and expected background particles among the candidates. For the present analysis $T_{\rm live}$ totaled 1286460 seconds. The effective geometrical acceptance including non-interaction efficiency ($S\Omega \cdot \varepsilon_{\rm non-int}$) was calculated using GEANT3 to be 0.133

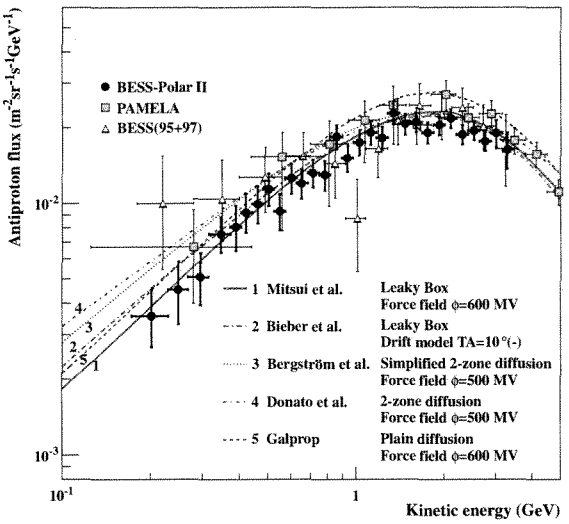

FIG. 2. Antiproton flux at the top of the atmosphere obtained with BESS-Polar II at solar minimum together with BESS flights around the previous solar minimum (BESS95+97) and PAMELA.

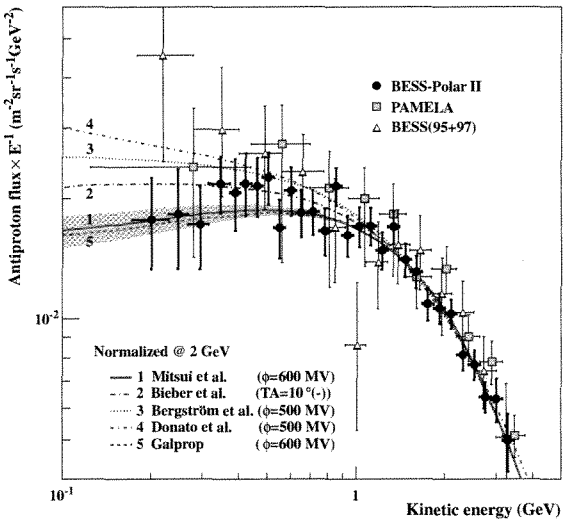

FIG. 3. Comparison of antiproton flux shapes with secondary $\bar{p}$ calculations. In order to focus on the difference of spectral shapes in the low-energy region, the calculations are normalized at the spectral peak $\sim$ 2 GeV. The uncertainty due to the modulation parametrization with the range from 500 MV to 700 MV in the Mitsui model is shown by the shaded band.

$\pm$ 0.011 m^{2}sr at 0.2 GeV and 0.159 $\pm$ 0.008 m^{2}sr at 2.0 GeV, with errors estimated from differences relative to GEANT4 calculations. The detection efficiency of $\bar{p}$'s ($\varepsilon_{\rm det}$) was calculated using a noninteracting proton sample to be 81.4 $\pm$ 0.1 % at 0.2 GeV and 60.0 $\pm$ 0.2 % at 2.0 GeV. Estimates of atmospheric secondaries included in $N_{\rm TOI}$ ($N_{\rm atmos}$) were calculated with the proton and helium fluxes measured by BESS-Polar II as input. The subtraction amounts to 17.6 $\pm$ 2.0 % at 0.2 GeV and 27.6 $\pm$ 0.1 % at 2.0 GeV, where the errors correspond to the maximum difference among three recent calculations [18–20]. In order to obtain the TOA flux, a correction for survival probability [19] in the residual atmosphere ($\varepsilon_{\rm air}$) was applied, and the probability was estimated as 85.6 $\pm$ 2.0 % at 0.2 GeV and 89.8 $\pm$ 2.0 % at 2.0 GeV.

Table I gives the resultant flux of $\bar{p}$'s at the top of the atmosphere in the kinetic energy range 0.17 to 3.5 GeV with the statistical (first) and systematic (second) errors. The dominant systematics come from atmospheric subtraction and detection efficiency. A rapid change in efficiency due to the ACC veto increases the systematic uncertainty in the two highest bins.

Shown in Fig. 2 is the BESS-Polar II $\bar{p}$ spectrum together with measurements by BESS95+97 and PAMELA, and various secondary $\bar{p}$ calculations [18, 21–24]. Improved statistical precision of the $\bar{p}$ flux measurement results from 14 and 30 times more events below 1 GeV than were measured in BESS95+97 and PAMELA [25], respectively. The $\bar{p}$ spectrum measured by BESS-Polar II generally shows good consistency with secondary $\bar{p}$ spectra calculated for solar minimum conditions.

The evident differences among the calculations shown in Fig. 2 arise from several factors: (1) definition of the primary proton and helium spectra, (2) incomplete knowledge of nuclear physics in propagation, (3) parameters and models of propagation in the Galaxy, and (4) the modulation in the heliosphere. These factors affect both the normalization and shape of a calculated $\bar{p}$ spectrum in different ways and degrees. Variation in the absolute fluxes of interstellar protons and helium will, for instance, affect the absolute flux of $\bar{p}$'s produced, but not the shape of the spectrum.

In Fig. 3, we normalize all of the $\bar{p}$ spectrum calculations near the peak energy at 2 GeV to focus on their shapes. The calculated spectra and data points are also multiplied by E_k^{-1} to further emphasize differences at low energies. *The data have not been normalized.* Precise measurement of the $\bar{p}$ spectrum to low energy by BESS-Polar II allows secondary $\bar{p}$ calculations to be evaluated by comparing predicted and observed spectral shapes. Chi-square (χ^2) calculated with BESS-Polar II data and normalized secondary $\bar{p}$ calculations in Fig. 3 are 0.57 (curve 1), 0.56 (curve 2), 1.24 (curve 3), 1.59 (curve 4), 0.63 (curve 5). The shaded band in Fig. 3, calculated using the Mitsui model [6] modulated with a standard symmetric approach (Force-Field), indicates the small variation that results from uncertainty in the modulation parameter. Shown is the range from 500 MV (lower border: χ^2=0.77) to 700 MV (upper border: χ^2=0.48). Even though Force-Field modulation over this range of parameters gives a visible change to the spectral shape, as does the Drift model, this is small in comparison to

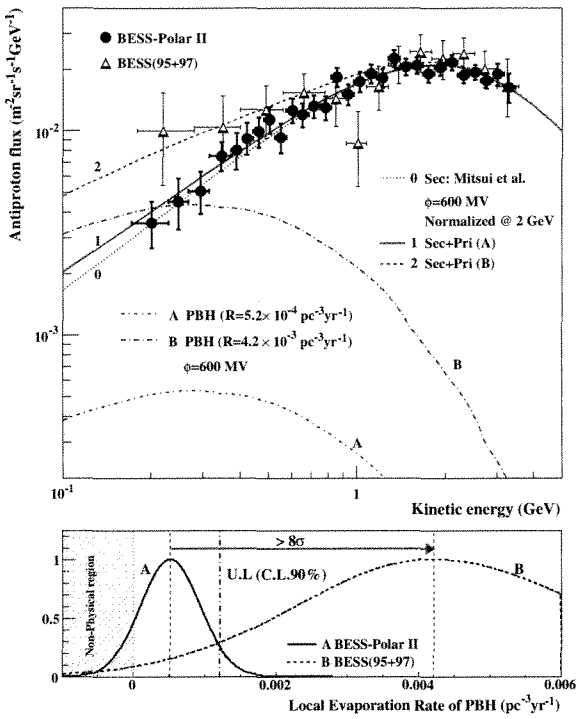

FIG. 4. (Top) Possible primary antiproton fluxes from evaporating PBHs calculated for BESS-Polar II (A) and BESS95+97 (B) by fitting differences of the measured spectra from the Mitsui secondary $\bar{p}$ spectrum. (Bottom) Distribution of the evaporation rate of PBH ($\mathcal{R}$) calculated for BESS-Polar II and BESS95+97. Negative values of $\mathcal{R}$ are non-physical.

variations among the propagation models, because of the shape of the low-energy $\bar{p}$ spectrum. BESS-Polar II results show better consistency with the models that do not include a component of low-energy $\bar{p}$'s from sources such as tertiary $\bar{p}$'s or a soft spectrum such as that due to the Diffusive Reacceleration model (curves 3 and 4 in Fig. 3).

Among the various possible sources of primary $\bar{p}$'s, the most pertinent candidate for BESS-Polar to study is the evaporation of PBHs that may have formed in the early Universe via initial density fluctuations, phase transitions, or the collapse of cosmic strings. PBHs are the only black holes that have small enough mass to emit particles with a significant "evaporation" rate at the current age of the Universe. The possible existence of primary $\bar{p}$'s has been quantitatively evaluated by focusing on the PBH evaporation rate parameter ($\mathcal{R}$) calculated by fitting the differences of $\bar{p}$ spectra measured in BESS-Polar II and BESS95+97 from theoretical secondary $\bar{p}$ calculations with normalization near the peak at 2.0 GeV. The normalization is performed to avoid bias from ambiguity in the absolute fluxes predicted by propagation models. The dependence on model choice is also considered by checking the primary $\bar{p}$'s under several models. The BESS-Polar II spectrum and the conservative models and modulations shown in Fig. 4 give $\mathcal{R} = 5.2^{+4.2}_{-4.1} \times 10^{-4}\mathrm{pc}^{-3}\mathrm{yr}^{-1}$. This excludes by 8 sigma the slight possibility of primary $\bar{p}$'s suggested by the $\mathcal{R}$ distribution with a mean value of $4.4 \times 10^{-3}\mathrm{pc}^{-3}\mathrm{yr}^{-1}$ determined from BESS95+97 data. We have also determined an upper limit of $\mathcal{R} \sim 1.2 \times 10^{-3}\mathrm{pc}^{-3}\mathrm{yr}^{-1}$ with a 90% confidence level. This upper limit is almost insensitive to the modulation used in the secondary model calculation (500 MV: $\mathcal{R} = 1.1 \times 10^{-3}\mathrm{pc}^{-3}\mathrm{yr}^{-1}$, 600 MV: $\mathcal{R} = 1.2 \times 10^{-3}\mathrm{pc}^{-3}\mathrm{yr}^{-1}$, 700 MV: $\mathcal{R} = 1.3 \times 10^{-3}\mathrm{pc}^{-3}\mathrm{yr}^{-1}$). Within statistics, the BESS-Polar II result shows no evidence of primary $\bar{p}$'s originating from the evaporation of PBH.

The BESS-Polar program is a Japan-United States collaboration, supported in Japan by the Grant-in-Aid 'KAKENHI' for Specially Promoted and Basic Researches, MEXT-JSPS, and in the U.S. by NASA. Balloon flight operations were carried out by the NASA Columbia Scientific Balloon Facility and the National Science Foundation United States Antarctic Program. We would like to express our sincere thanks for their continuous professional support.

* Present address: ICRR, Tokyo
† Present address: INFN, Perugia
‡ Present address: Tokushima University
§ Corresponding author; Present address: NASA-Goddard Space Flight Center; Kenichi.Sakai@nasa.gov

[1] T. K. Gaisser *et al.*, Astrophys. J., **394** 174 (1992).
[2] K. Yoshimura, Adv. Space Res., **27** 693 (2001).
[3] A. W. Strong *et al.*, Astrophys. J., **613** 962 (2004).
[4] S. W. Hawking, Commun. Math. Phys., **43** 199 (1975).
[5] K. Maki *et al.*, Phys. Rev. Lett., **76** 3474 (1996).
[6] T. Mitsui *et al.*, Phys. Lett., **B389** 169 (1996).
[7] S. Orito *et al.*, Phys. Rev. Lett., **84** 1078 (2000).
[8] A. Yamamoto *et al.*, Adv. Space Res., **30** 1253 (2002).
[9] J. W. Mitchell *et al.*, Nucl. Phys. (Proc. Suppl.), **134** 31 (2004).
[10] T. Yoshida *et al.*, Adv. Space Res., **33** 1755 (2004).
[11] A. Yamamoto *et al.*, Adv. Space Res., **42** 442 (2008).
[12] K. Yoshimura *et al.*, Adv. Space Res., **42** 1664 (2008).
[13] M. Sasaki *et al.*, Adv. Space Res., **42** 450 (2008).
[14] K. Abe *et al.*, Phys. Lett., **B670** 103 (2008).
[15] Y. Ajima *et al.*, Nucl. Instrum. Meth., **A443** 71 (2000).
[16] S. Haino *et al.*, Nucl. Instrum. Meth., **A518** 167 (2004).
[17] S. Haino *et al.*, Phys. Lett., **B594** 35 (2004).
[18] T. Mitsui, Ph.D. thesis, University of Tokyo.
[19] S. A. Stephens, Astropart. Phys., **6** 229 (1999).
[20] K. Yamato *et al.*, Phys. Lett., **B632** 475 (2006).
[21] J. W. Bieber *et al.*, Phys. Rev. Lett., **83** 674–677 (1999).
[22] L. Bergstrom *et al.*, Astrophys. J., **526** 215 (1999).
[23] F. Donato *et al.*, Astrophys. J., **563** 172 (2001).
[24] V. S. Ptuskin *et al.*, Astrophys. J., **642** 902 (2006).
[25] O. Adriani *et al.*, Phys. Rev. Lett., **105** 121101 (2010).